Transport Estimates from Altimeter Data in the South Atlantic Ocean

Edzard Romaneessen GeoForschungsZentrum Potsdam, Dept. 1, D-PAF, D-82230 Oberpfaffenhofen
eroman@dfd.dlr.de
http://www.gfz-potsdam.de/

Abstract

Collinear analyzed SSH from ERS-1 and Topex, the free surface of the parallel ocean general circulation model (POCM) by *Semtner and Chervin (1992)* and monthly dynamic topography calculated from *Levitus et al., (1994)* data is used to study the seasonal gyre circulation in the South Atlantic. Of all data sets the annual harmonic component of one year is computed for comparison purpose. In addition, the SSH variations from altimetry are combined with a hydrographic data set in a simple diagnostic 2-layer transport model. From this the upper layer transport estimates are compared with upper layer transports derived from the POCM velocity field.
Both, SSH and transport comparisons give a strong hint on a seasonal circulation of the subtropical gyre, being strongest during austral fall. The general good agreement between POCM and altimetry indicates that this signal is due to buoyancy forcing in the mixed layer. Equally good agreement could not be achieved between the monthly Levitus dynamic topography and the altimeter data. This is probably due to the inaccuracy of the Levitus data in this region.

Keywords: Altimetry, ERS-1, Topex, SSH, dynamic topography, current transport, POCM, Levitus, seasonal variability

1 Introduction

The upper layer circulation of the South Atlantic is made up of a complex range of flows at a variety of spatial scales as the schematic representation of the currents in Figure 1 [after *Peterson and Stramma, 1991*] shows. But nevertheless, the broad subtropical gyre flow is the dominating feature of the South Atlantic. It consists of four different parts: (1) the westward Southern South Equatorial Current (SSEC) to the north, (2) the southward Brazil Current to the west, (3) the eastward South Atlantic Current (SAC) to the south and (4) the northward Benguela Current to the east. This subtropical gyre is known to be basically wind driven in its mean part. But until now it is quite unclear whether there is a seasonal varying gyre circulation and how this is forced.

In order to address this question, this study uses ERS-1 and Topex altimeter data, as well as data from the general circulation model by *Semtner and Chervin (1992)* and temperature and salinity data from *Levitus et al (1994)* to investigate, whether a seasonal signal, seen in the SSH of the South Atlantic from altimetry can be related to transport variations in the mixed layer of the subtropical gyre. As a possible driving mechanism, seasonal buoyancy fluxes are discussed in context with investigations made by *Wang and Koblinsky (1996)* for the North Atlantic and North Pacific. There, a seasonal signal seen in the sea surface height (SSH) from altimetry is related to a seasonal signal in the subtropical recirculation cell driven by seasonal varying buoyancy fluxes into the mixed layer.

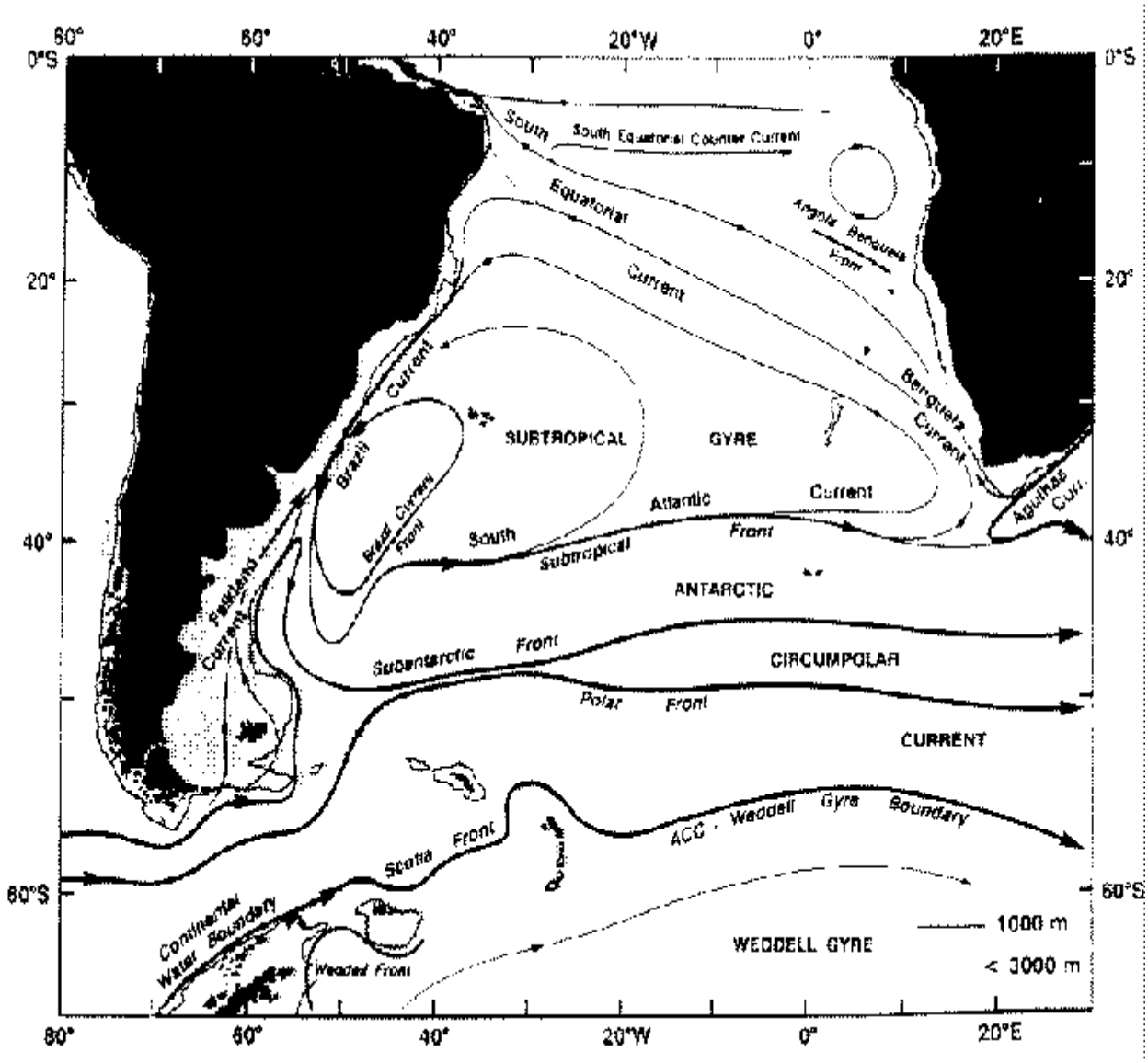

Figure 1: Mean upper circulation of the South Atlantic (after Peterson and Strammer, 1991)

2 Data Description

Altimeter data

For this study, the first overlapping year (Nov. 92 - Nov. 93) of precise altimeter products from the European ERS-1 mission and the joint French/U. S. TOPEX/POSEIDON (T/P) mission are used. During that time, the multidisciplinary phase, the ERS-1 went in an 35 day repeat cycle while T/P was continuously operating in a 10 day repeat cycle. Both data sets (ERS-1 and Topex; no Poseidon data is used) are processed in the same way as shown in the flow diagram (Figure 2). On the right hand side in Figure 2 the processing step is shown leading to a certain type of data seen on the left hand side.

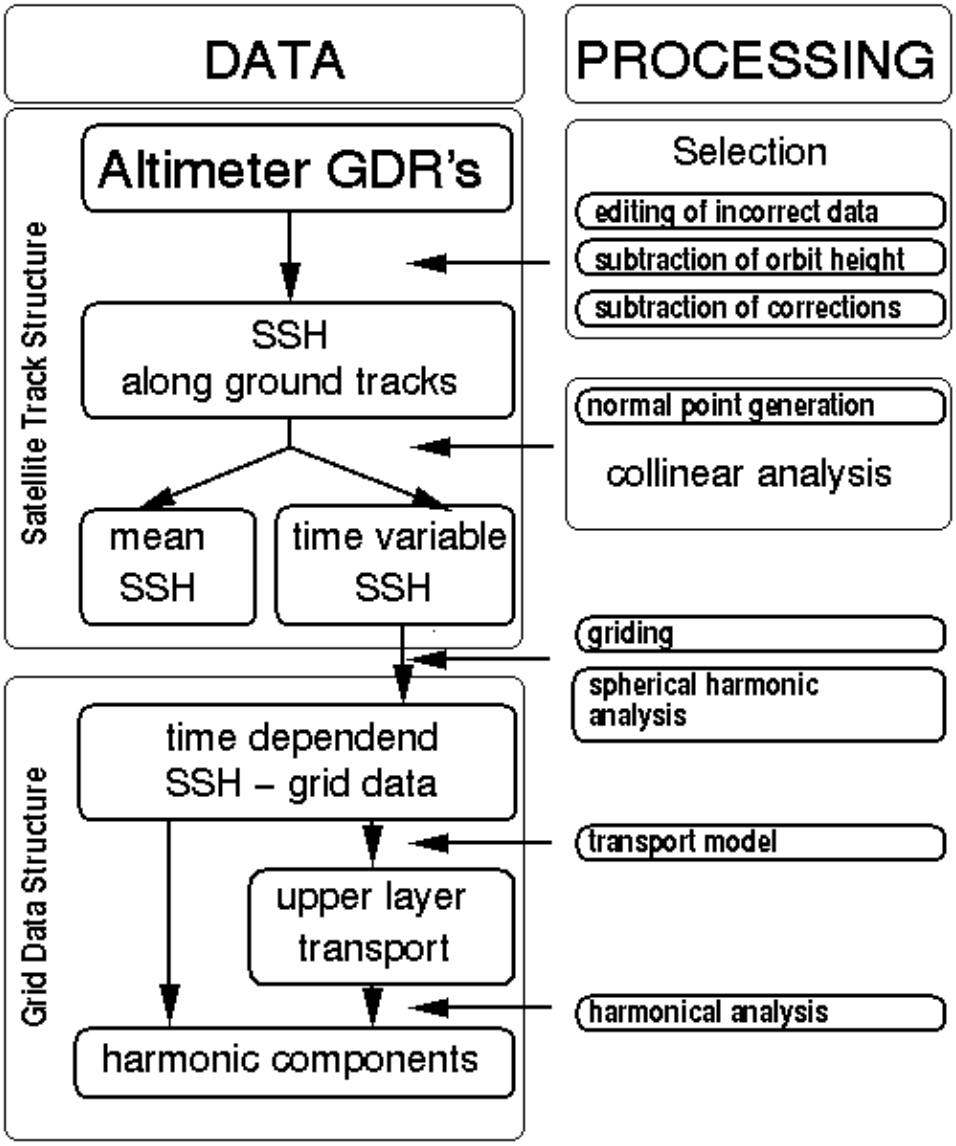

Figure 2: Flow diagram of altimeter data processing

As a first step, data selection is performed. From both ERS-1 and Topex, data in the region (10°N - 60°S; 70°W - 30°E) is selected and bad data (sigma range > 0.75m , SWH > 10m, wind speed > 12 m/s) excluded. Then 11 ERS-1 35 day cycles (07. Oct.'92 - 01. Nov '93) and 37 Topex 10 day cycles (01. Nov 92 - 03. Nov 93) have been selected, to get approximately one year of full cycles for each satellite.

All altimeter data is corrected using the following methods/models [if different, the Topex corrections are in parenthesis]: orbit height with TEG-3 (JGM-2), sea state bias according to *Gaspar and Ogor (1994)* [*Fu and Glazmann, 1991*], inverse barometer, FES95.2.1 ocean tides by *Le Provost et al. (1996*), earth tide by *Wahr (1981) [Cartwright and Taylor, 1971]*, IRI95 ionosphere by *Bilitza (1996)* [dual frequency], wet troposphere from radiometer and FMET [ECMWF] dry troposphere. In addition, the original ERS-1 OPR02 data is corrected for time tagging, SPTR and USO drift as described by *Gruber et al. (1997)*.

With these two corrected data sets a collinear analysis was performed to get along-track sea surface height (SSH) deviations from the mean. No additional orbit error corrections were applied to the data.

All SSH-anomalies are interpolated on a 0.5° x 0.5° grid of 12 monthly maps for ERS-1 and 37 10 day maps for Topex in two steps. First, a weighted mean interpolation with an influence circle of 4, a half weight width of 2and no weighting in time is performed. In a second step, the small scale eddy signal is filtered by means of a spherical harmonic analysis up to degree and order 40 (500 km half wave length).

Additional data

This study is based on two additional data sets. Firstly, the objectively analyzed and 1°x 1° grided monthly mean historical temperature (T) and salinity (S) fields from *Levitus et al (1994)* and *Levitus and Boyer (1994)* .

The data is used to compute monthly mean dynamic topography to be compared with the SSH anomalies from altimetry (see section 4). In addition, the T, S fields are used to computed the three dimensional geostrophic velocity field relative to 1000dbar, which leads to the upper layer transport by integration between 0 and 500m (see section 5). A further application is the determination of the mixed layer depth. The mixed layer depth is used to make transport estimates from altimetry as described in section 3

The second data set used for comparison is from the Parallel Ocean Circulation Model (POCM) by *Semtner and Chervin (1992).* The data is from the model run POCM_4B which covers the time period 1987 - 1994, forced by ECMWF surface fields as described in detail by *Stammer et al. (1996).* It is worth mentioning, that in this model run monthly ECMWF surface heat fluxes are incorporated into the first model layer. The model has a Mercator grid with a resolution of 0.4° in

longitude and 0.4° *cos(phi) in latitude. It has 20 depth levels with layer thickness between 25m in the upper layer and 550m in the deep layers. From the model data, the monthly mean horizontal velocity component u is used to calculate the model transport across 30°W. In addition, the monthly free surface anomaly eta' of the model is compared to SSH anomalies from altimetry . Therefore, the resolution is reduced to 0.5° x 0.5° and a spherical harmonic analysis up to degree and order 40 is performed. For comparison purpose, only data that cover the same time span as the altimeter data (Nov '92 - Oct '93) have been selected.

3 Method of transport estimation

In order to derive transport estimates from the SSH anomalies received from altimetry, a simple 2-layer approximation is used. Following *Goni et al. (1995),* the baroclinic upper layer transport is:

$$T_{ul}(t) = \frac{g \times \epsilon}{f}\left(h(t)^2_{1,right} - h(t)^2_{1,left}\right) \qquad (1)$$

with:

$$\begin{aligned} h^2_{1,i} &= (\bar{h}_{1,i} + h'_{1,i}(t) + \eta'_{1,i}(t))^2 \\ &= (\bar{h}_{1,i} + (1 + 1/\epsilon_i)\eta'_{1,i}(t))^2 \qquad (2) \\ \epsilon &= (\rho_2 - \rho_1)/\rho_2 \qquad (3) \end{aligned}$$

where g is the earth gravity, f the coriolis force and epsilon is the reduced density calculated from the upper (rho1) and lower (rho2) layer density. h1, h1' are the mean and the variable part of the upper layer depth and eta' is the SSH anomaly from altimetry. Thus, the baroclinic upper layer transport can be calculated from the altimetric SSH anomaly, if the mean mixed layer depth and the reduced density is known.

The mixed layer depth is estimated from the *Levitus et al (1994)* data for each month by defining it as the minimum depth at which the temperature is 1°C colder than the surface temperature. The mixed layer depth shown in Figure 3 is then chosen to be the average depth of all months, which is between 60 and 110 m in the South Atlantic.

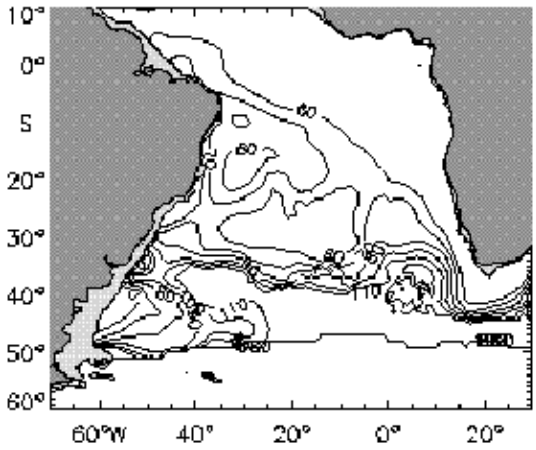

Figure 3: Mixed layer depth in the South Atlantic from Levitus temperature data

The reduced density epsilon is calculated by taking the density of the surface layer from the Levitus data as rho1 and the density of the next layer below the thermocline depth as rho2 in equation (3) for each month. From these monthly epsilon, again the average is taken for the transport calculation with equation (1).

4 Sea Surface Variability

Usually, the SSH-variability from altimeter data is computed by taking the along-track variability of each track around its mean from collinear analysis and interpolating it on a regular grid with some influence radius (e.g. 4°) and half weight radius (e.g. 2°) [e.g. *Nerem et al., 1994].* Doing so for ERS-1 and TOPEX both are in general good agreement. The minimum values in the silent region of the South Atlantic, which is called the noise level, are slightly above 3 cm for TOPEX and around 4 cm for ERS-1, i.e. the ERS-1 values are generally higher. Another way of determining the variability is to take the individual along track deviation from mean of each track and interpolate it onto a regular grid with an average of zero and standard deviation representing the sea surface height variability as shown in Figure 4. The advantage of this method is that in both (ERS-1 and Topex) grid interpolations about the same number of data is included since both satellites have about the same ground velocity. In Figure 4, the minimal values close to the equator as well as the maximal values in the Brazil/Falkland Confluence and the Agulhas Retroflection are of the same order. But in the region between minimum and maximum, the ERS-1 values are higher. This can also be seen in the annual harmonic component. The reason for these differences could be due to some different corrections, but its more likely that the reason is to be found in the different sampling which might be advantageous for ERS-1 in low variable areas.

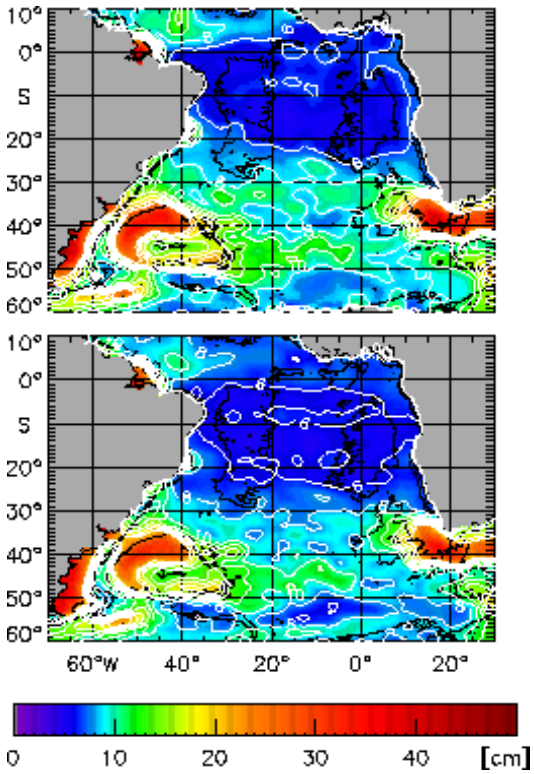

Figure 4: Total variability from collinear analyzed ERS-1 and Topex data

The comparison of the annual harmonic component of the grided SSH-anomalies reveals the same higher amplitudes for ERS-1 in that area. This can bee seen in Figure 5 where the harmonic components of all datasets are shown as amplitude of a cosines in centimeters and phase of the maximum amplitude in month. Between ERS-1 and Topex the amplitude and some what less the phase compare even in details very good, except that ERS-1 is about 1-2 cm higher in the central South Atlantic. From this analysis, there are from north to south four different areas to be distinguished:

Directly north of the equator, the North Equatorial Countercurrent (NECC) area, with maximum amplitudes in September/October, which comes from the annual NECC retroflection due to the movement of the ITCZ [see e.g. *Didden and Schott, 1992]*.

The area of the seasonal varying equatorial branch of the South Equatorial current(SEC), visible in the amplitude gradient between almost zero along 3^oS and the higher amplitudes to the south of it. The phase shows a strong gradient along this line as well, leading to maximum SEC currents in May/June.

The area of the triangular shaped subtropical gyre, visible as higher amplitudes in the central South Atlantic region, leaned against the South American coast. The phase in this area shows maximum amplitudes in February/March. The boundary is most pronounced to the northern side, where a strong gradient in amplitude and phase along the line 10^oS, 35^oW - 30^oS, 0^oE exist. To the south, the boundary is between 40^o and 45^oS but less well pronounced.

South of the subtropical gyre, the amplitudes are very low, except for the Drake Passage region in the west. The phases are around September/October.

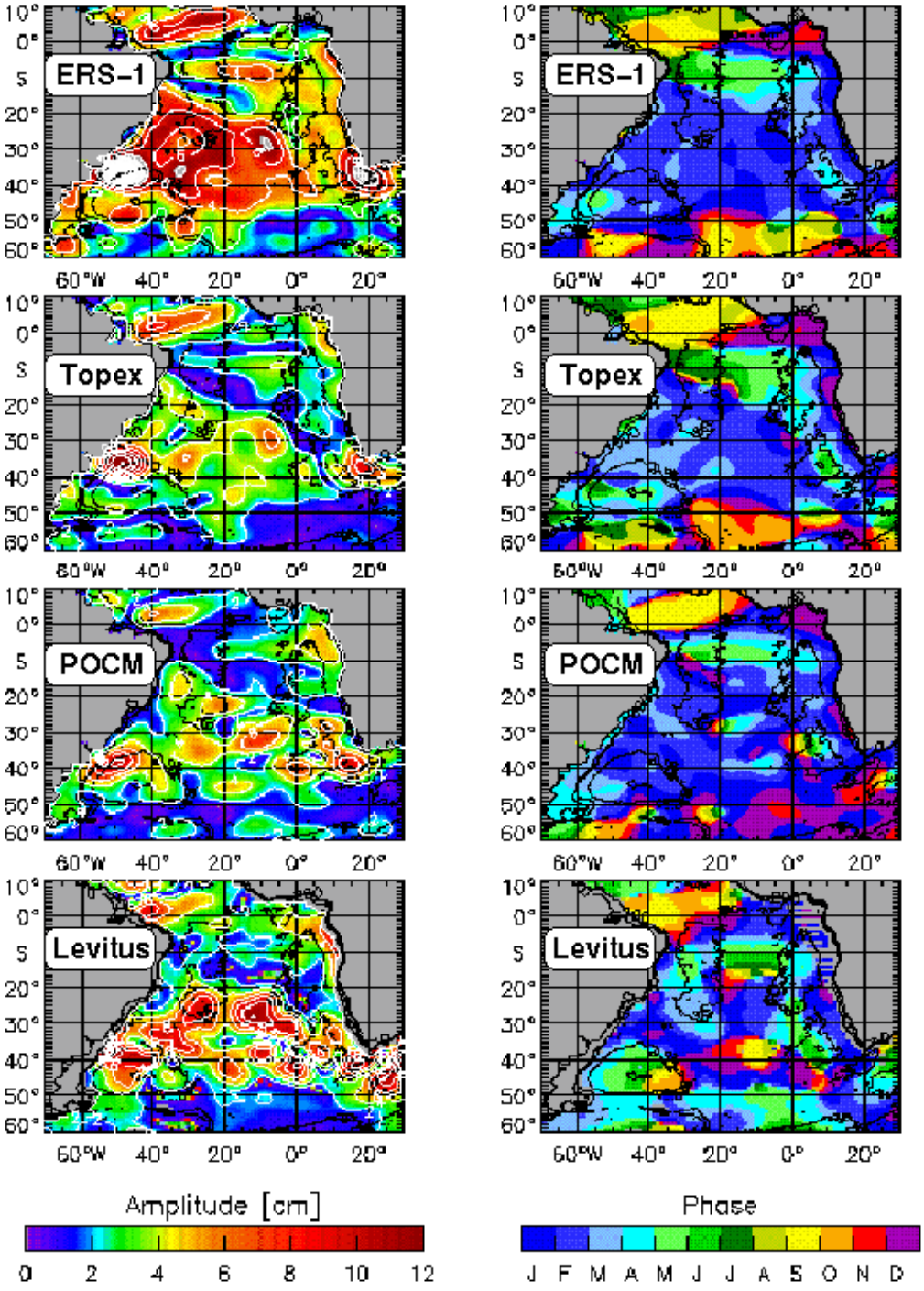

Figure5: Annual harmonic SSH from ERS-1, Topex, POCM and Levitus dynamic topography

From this four areas, the main interest of this study is focused on the seasonal signal in the subtropical gyre. This signal is believed by the author to present a seasonal gyre circulation with maximum transport in austral fall, comparable to those described in a recent study of *Wang and Koblinsky (1996)* for the subtropical recirculation in the North Atlantic and North Pacific. The possible driving mechanism are discussed in context with other investigations as follows:

As described by *Gill and Niiler (1973)* the seasonal sea surface height anomaly primarily consists of a baroclinic part caused by changes in the steric height in the upper 200 m due to buoyancy forcing and a barotropic part driven by seasonal windstress forcing. In a recent study of the seasonal variability in the South Pacific subtropical gyre *Morris et al. (1996)* considered the latter as a possible mechanism of the observed annual intensification of the gyre scale circulation. Their transport estimates from XBT measurements showed a maximum in November and a Ekman pumping leading this signal by about 3 months.

In the southwestern Atlantic *Matano et al .(1993)* showed that changes in the subtropical gyre transport are as well related to windstress variations, using a barotropic model. But their investigation area was limited to southward of 25S and their argumentation based upon a higher seasonal cycle in the windstress southward of 35S. Whereas from the analysis of the COADS data can bee seen, that northward of 25S, the windstress is stronger in austral winter (see *Hasse et al..1996,* their figure 2.13). This implies that at least for the northern part of the subtropical gyre, the annual varying wind field is not the primary forcing mechanism.

Thus, if wind stress is not the primary driving mechanism, it must be the buoyancy forcing (i.e. air-sea net heat and fresh water flux). This can be confirmed by comparison between the altimeter and the POCM data (see Figure 5). The general pattern of the annual harmonic SSH variation is in good agreement between model and altimetry even if the model signal is some what less. But, as stated by *Stammer et al. 1996* this good agreement could not be obtained from an earlier model run, where no sea surface fluxes have been included into the model (see model data). Thus, the achieved good agreement leads to the assumption, that this signal is mainly driven by surface buoyancy fluxes into the mixed layer.

Generally, this should be provable by investigating the Levitus data, which are based on *in situ* measurements. But as can be seen in Figure 5 , the annual harmonic of the Levitus dynamic topography is much noisier especially in the strongly varying phase. The amplitude is in rough agreement showing higher values in the subtropical gyre. But the triangular shaped subtropical gyre structure does not come out clearly. This is probably due to the lack of sufficient hydrographic data in the

southern oceans, that make up this dataset. Because of the noisiness, it was not possible to evaluate a proper seasonal signal in the mixed layer depth from the Levitus data. This seasonal mixed layer signal was used by *Wang and Koblinsky (1996)* in the North Atlantic as a prove that the seasonal gyre circulation is basically confined in the mixed layer and driven by buoyancy fluxes. Instead, a simple two layer assumption is made to calculate the variable mixed layer depth and volume transport from equation (3) from altimeter data. The results of this transport estimates are compared between all datasets in the following section.

5 Transport across 30°W

To have a connection to the mean circulation of the South Atlantic subtropical gyre sketched in Figure 1 , Figure 6 shows the mean zonal transport from the Levitus data across 30° W. This transport is calculated by integrating the geostrophic velocity between 0 and 500 m. The geostrophic velocitys are calculated relative to 1000 dbar, because the monthly values exist only to this depth. Figure 6 clearly shows the westward northern branch of the subtropical gyre which is the Southern SEC (SSEC) northward of 26°S and the eastward southern branch, which is the SAC both shown in Figure . An integration between 10°and 20°S leads to a mean westward transport in the SSEC of 19.5 Sv (1Sv =$10^{o}m^{o}$ / s), which is comparable to transports found by *Stramma (1991),* whereas the mean zonal transport in the upper 550m from the POCM data reveals only 11.5 Sv because the model has some eastward countercurrents in this part of the 30W section.

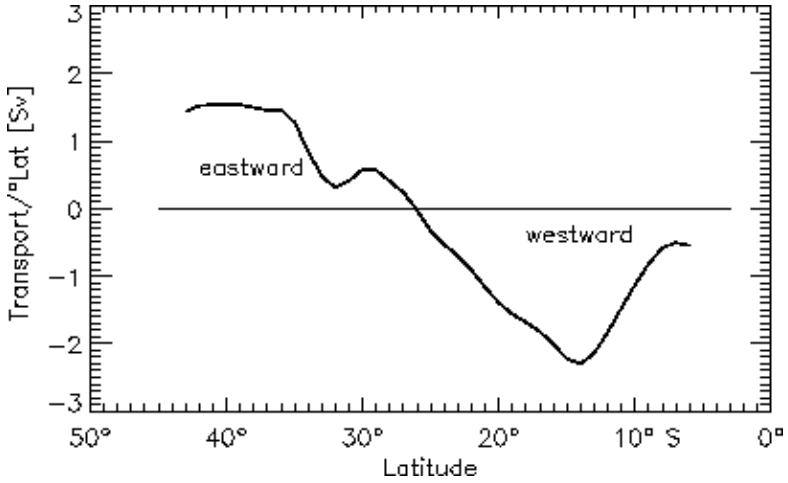

Figure 6: Mean geostrophic transport per degree Latitude of the upper 500m from Levitus data

The same latitude section [10°- 20°S] was taken to compute the time variable part of SSEC, as shown in Figure . The transports from altimetry are computed as described above, the transports from Levitus and POCM are computed in the same way as for the mean part. From each dataset the mean value is subtracted. The mean of the mixed layer transport from altimetry is about zero and for the other two as given above. Except of Levitus, all data have the time span Nov. 92 - Oct '93, which is simply shifted for better comparison purpose. As can bee seen, all transport calculations, except those from the Levitus data, show a fairly well pronounced seasonal cycle with maximum westward transports in austral fall, i.e. around March and minimum - maximum difference of 3-4 Sv.

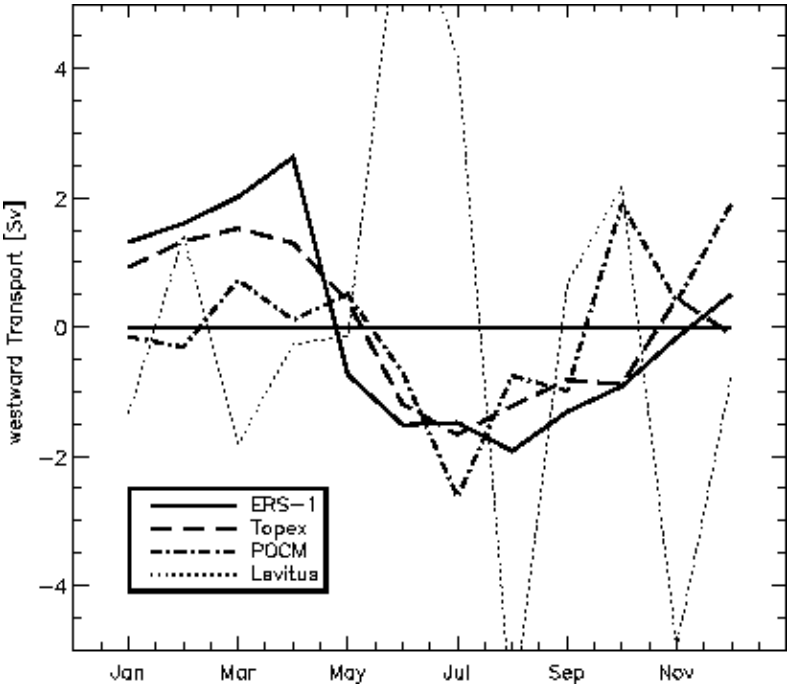

Figure 7: Time variable transport across 30 W integratet between 10S and 20S. Positive values result in stronger westward transport of the Southern SEC.

The seasonal transport for the eastward part of the subtropical gyre which is not shown here is much less pronounced. Best results along 30°W have been achieved by integrating between [37°- 43°S]. The maximum eastward transport is again in austral fall, fitting in the assumption of a stronger gyre circulation during that time. But the minimum - maximum difference between austral spring and austral fall is only about 1 Sv.

Despite of this rather small seasonal signal in the eastward South Atlantic Current (SAC), the concept of a seasonal varying gyre circulation is supported by two additional aspects. First, the Brazil/Falkland Confluence (see Figure 1) is known to vary seasonally, being further south during austral summer than during austral winter [*Olson et al. ,1988*]. The reasons are currently under discussion, including a seasonal varying wind field [*Matano et al. 1993*] as well as stronger Brazil Current advection.

The other aspect is a recent investigation of *Stramma and Schott (1996).* They found an undercurrent, called the North Brazil Undercurrent (NBUC) off the Brazil Coast at 10°S as well as at 5°30' S. This NBUC shows a northward transport of more than 22 Sv in the upper 1000m. From historical data near 10°S, they found a seasonal signal in the NBUC being larger in austral spring (22.2 Sv in Nov'92) than in austral fall (17.1 Sv in Mar '94). This signal reduction of the northward NBUC during fall could be explained by a stronger southward gyre circulation in that time.

7 Conclusion

The annual harmonic signal of the South Atlantic sea surface height has been analyzed from four different sets of data. These are in generally good agreement showing a in amplitude and phase visible signal in the region of the triangular shaped subtropical gyre. From comparison between the SSH from altimetry and POCM it can be concluded that this signal is a result of the buoyancy forcing in the mixed layer (see discussion in section 4). In addition, this signal is believed to be related to a seasonal circulation of the whole subtropical gyre, being stronger during austral fall than during austral spring. The idea is supported by a simple two layer model. It is used to compute seasonal varying transports from altimeter data in the mixed layer of the subtropical gyre. The seasonal transport variations found with this method are the same order in amplitude and phase as transports calculation from the POCM data.

References

Bilitza, D., 1996, *International Reference Ionosphere 1995*, personal communications

Cartwright, D., and R. Tayler, New computations of the tide-generating potential, *Geophys. J. Royal Astronomic Society*, **23**, 45-74, 1971

Didden, N., and F. Schott, Seasonal variations in the western tropical atlantic: Surface circulation from geosat altimetry and woce model results., *Journal of Geophysical Research*, **97**, No. C3, 3529-3541, 1992

Fu, L.-L., and R. Glazmann, The effect of wave age on the sea state bias in radar altimetry measurement, *Journal of Geophysical Research*, **96**, 8829-8834, 1991

Gaspar, P., and F. Ogor, *Estimation and analysis of sea stae bias of the ERS-1 altimeter*, Technical report, Report of Task B1 - B2 of IFREMER Contract, 1994

Gill, A. E., and P. P. Niiler, The theory of seasonal variability in the ocean, *Deep-Sea-Research*, **20**, 144-177, 1973

Goni, G., S. Kamholz, S. Garzoli, and D. Olson, Dynamics of brazil/malvinas confluence based on inverted echo sounders and altimetry, *Journal of Geophysical Research*, **submitted**, 1995

Gruber, Th., M. Anzenhofer ,M. Rentsch, **E. Romaneessen**, Improvement of D-PAF Altimeter Products, in *Proceedings of 3rd ERS Symposium, 17-21 March 1997, Florence, Italy*

Hasse, L., R. Lindau, and E. Ruprecht, *The Warm Water Sphere of the North Atlantic*, Chapt. 2: Climatological Fluxes at the Sea Surface, Gebrü der Borntraeger, 1996

Le Provost, C., F. Lyard, J. M. Molines, M. L. Genco, and R. F., A hydrodynamic ocean tide model improved by assimilating a satellite altimeter derived dataset, *Journal of Geophysical Research*, **submitted**, 1996

Levitus, S., and T. Boyer, *World Ocean Atlas 1994 Volume 4: Temperature*, Technical report, U. S. Department of Commerce, Washington, 1994

Levitus, S., R. Burgett, and T. Boyer, *World Ocean Atlas 1994 Volume 3: Salinity*, Technical report, U. S. Department of Commerce, Washington, 1994

Matano, R. P., M. G. Schlax, and D. B. Chelton, Seasonal variability in the southwestern atlantic, *Journal of Geophysical Research*, **98(C10)**, 18027-18035, 1993

Morris, M., D. Roemmich, and B. Cornuelle, Observations of variability in the south pacific subtropical gyre, *Journal of Physical Oceanography*, **26**, No. 11, 2359-2380, 1996

Nerem, R., E. Schrama, C. Koblinsky, and B. Beckley, A preliminary evaluation of ocean topography from the topex/poseidon mission, *Journal of Geophysical Research*, **99**, 24565-24583, 1994

Olson, D. B., G. P. Podest, R. H. Evans, and O. B. Brown, Temporal variations in the separation of brazil and malvinas currents, *Deep-Sea-Research*, **35(12)**, 1971-1990, 1988

Peterson, R. G., and L. Stramma, Upper-level cirulation in the south atlantic, *Progress in Oceanography*, **26**, 1-73, 1991

Semtner, A. J., and R. M. Chervin, Ocean genral circulation from a global eddy-resolving model, *Journal of Geophysical Research*, **97**, No. C4, 5493-5550, 1992

Stammer, D., R. Tokmakian, A. Semtner, and C. Wunsch, How well does a 1/4global circulation model simulate large scale oceanic observations?, *Journal of Geophysical Research*, **101**, No. C10, 25779-25811, 1996

Stramma, L., Geostrophic transport of the south equatorial current in the atlantic, *Journal of marine Research*, **36**, 639-646, 1991

Stramma, L., and F. W. Schott, *The Warm Water Sphere of the North Atlantic*, Chapt. 7: Western Equatorial Circulation and Interhemispheric Exchange, Gebr"uder Borntraeger, 1996

Wahr, J., Body tides on an elliptical, rotating elastic and oceanless earth, *Geophys. J. R. Astr. Soc.*, **64**, 1981

Wang, L., and C. J. Koblinsky, Annual variability of the subtropical recirculation in the north atlantic and north pacific: A topex/poseidon study, *Journal of Physical Oceanography*, **26**, No. 11, 2462-2479, 1996